International Journal of Thermophysics, Vol. 9, No. 5, 1988

Thermal Expansion Properties of 6061 Al Alloy Reinforced with SiC Particles or Short Fibers[1]

T. A. Hahn[2] and R. W. Armstrong[3]

Thermal expansion measurements are reported for 6061 Al alloy and drawn composite materials reinforced with SiC particles or aligned short fibers. Samples with volume fractions of 5 and 20% SiC were measured in the drawing direction. The measurements were obtained from repeated heating and cooling cycles between room temperature and 500°C. Cumulative plastic strains were measured for the repeated thermal cycles, in association with the observation that lower expansivities generally occurred on cooling as compared with heating. Model calculations for particulate and an aligned fiber are presented for the combined elastic–plastic deformation properties of the Al/SiC composite systems. Lower expansivities and greater plastic strains are accounted for in the fiber-reinforced material.

KEY WORDS: 6061 Al–SiC composites; coaxial cylinder model; elastic–plastic concentric-spheres model; expansivities; thermal cycling; thermal expansion; thermal stresses; thermally induced plasticity.

1. INTRODUCTION

The thermal expansion properties of several eutectic aluminum (Al)–silicon (Si) alloys have been investigated on the basis of modeling the system as a metallurgical composite [1]. The Al–Si alloy was chosen because earlier X-ray measurements indicated that appreciable thermal stresses occurred between the phases [2]. Model calculations had indicated further that large plastic strains should have occurred within the Al phase [2, 3].

---

[1] Paper presented at the Tenth Symposium on Thermophysical Properties, June 20–23, 1988, Gaithersburg, Maryland, U.S.A.

[2] Composites and Ceramics Branch, Naval Research Laboratory, Washington, D.C. 20375, U.S.A.

[3] Department of Mechanical Engineering, University of Maryland, College Park, Maryland 20742, U.S.A.

0195-928X/88/0900-0861$06.00/0

Silicon carbide (SiC) has a thermal expansivity comparable to that of Si, and Al–SiC composite materials are of interest for their ease of fabrication, strength, and elastic stiffness properties. Figure 1 shows the thermal expansions measured for Al–0.20 SiC, by volume, particle, or whisker systems in comparison with that for Al, Si, and SiC over the temperature range from 20 to 500°C. The $(\Delta L/L)$ and $(\Delta a/a)$ curves were reported for pure Al in a pioneering study to determine the concentration of lattice vacancies as a function of temperature [4]. The results obtained here for 1100 Al fit the pure Al curve. The lowered curves computed for Al with its equilibrium solid solubility of Si at each temperature and, also, that for 6061 Al show that the thermal expansion property is reasonably sensitive to relatively low concentrations of alloying elements.

The effect of the 20% (by volume) of particles on reducing the thermal expansion of 6061 Al below its normal value can be seen in Fig. 1 to be greater than that which would be obtained on a volume-averaged rule of mixtures basis, that is, the experimental points for the particle composite clearly fall below 0.80 of the expansion values shown for the 6061 Al. The (axial) expansion reduction is significantly greater even for the 20% whisker material. In both cases, the greater than proportionate reduction in expansion property can be traced to the generation of thermal stresses in the composite systems. This has been the main concern of the present investigation.

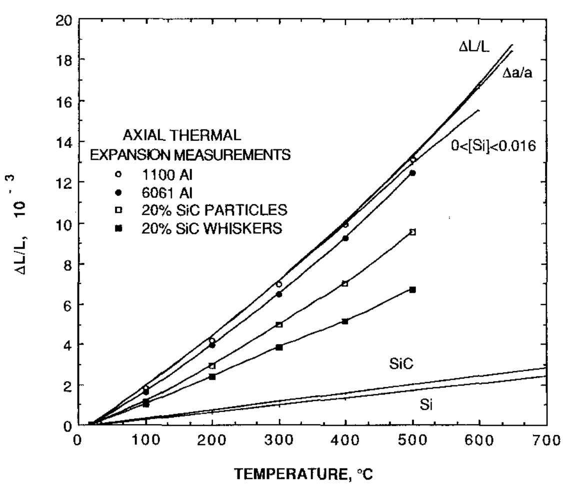

Fig. 1. Average thermal expansion as a function of temperature of pure Al [4], 1100 Al, Si-saturated Al solid solution, Si, SiC, 6061 Al, and 6061 Al–0.20 SiC particle or whisker systems.

2. EXPANSION MEASUREMENTS

Accurate length measurements were obtained on both heating and cooling at 20°C, at 100°C, and at 100°C intervals extending to 500°C on four 6061 Al–SiC composites and the 6061 Al alloy. Four composites of 5 and 20 vol% SiC in 6061 Al and also the 6061 Al alloy itself were supplied from a previous study [5] of the mechanical properties of these materials, also giving microstructural details. Samples with 5 and 20% discontinuous fiber or whisker SiC reinforcement had been manufactured by ARCO SILAG in the form of extruded rods 8 mm in diameter. Other samples were manufactured by DWA Composite Specialists with 5 and 20% particles or platelet SiC, also in the form of extruded rods. Measurements were carried out parallel to the extrusion direction for all of the materials.

Expansion measurements were obtained with a fused quartz dilatometer [1]. Sensitivities of 0.1°C in the temperature measurements and 1.0 μm in the length measurements were achieved. A sample length of 50 mm gave an expected uncertainty in the expansivity values of about 1%. The system was calibrated according to ASTM Test Method E-228 [6] with a pure platinum sample. The platinum sample was run periodically to ensure the constancy of the correction values used for calculating the thermal expansion properties. A previous analytical equation [7] was used to calculate the platinum expansion at each experimental equilibrium temperature. An expansion correction for the enclosing fused quartz tube of $\Delta L/L = 0.24 \times 10^{-3}$ at 500°C, compared with a total correction of $\Delta L/L = 0.35 \times 10^{-3}$, was the main contribution to correcting the measurements. Agreement of the expansion values for 1100 Al with the previous pure Al measurements [4] was found to be reproducible over three complete thermal cycles as indicated in Fig. 1. The lower expansion of the 6061 Al alloy compared with the 1100 Al material is attributed to the low expansion of the 1.0 Mg, 0.6 Si, 0.3 Cu, and 0.2 Cr (by wt%) alloying elements which are nominally contained in the 6061 Al material.

Figure 2 shows, on a basis comparable to Fig. 1, the average expansion measurements on 5 and 20% SiC whisker reinforcement added to the 6061 Al alloy. The pronounced effects of the SiC whisker geometry on reducing the composite expansion is evident from the fact that the 5% whisker result shown in Fig. 2 is very nearly the same as was achieved with 20% particles shown in Fig. 1. From a volume-average calculation involving the 6061 Al and SiC expansions shown in Fig. 2, an expected expansion for the 5% whisker sample would be approximately $\Delta L/L = 11.9 \times 10^{-3}$ at 500°C; the measured result is significantly smaller, at $\Delta L/L = 9.47 \times 10^{-3}$, as shown in Table I. This mismatch is far greater for the 20% SiC whisker composite, where an expansion of $\Delta L/L = 10.34 \times 10^{-3}$ is calculated on a

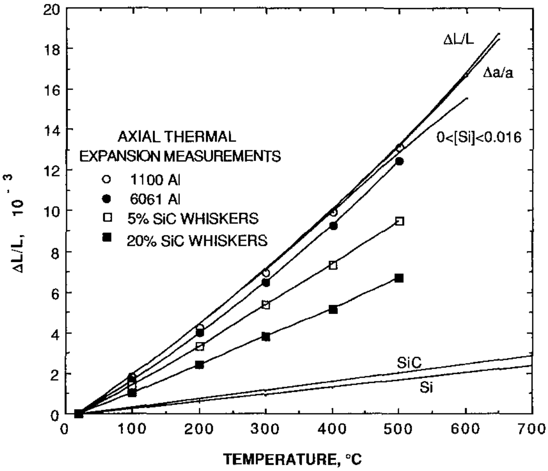

Fig. 2. Average thermal expansion as a function of temperature of pure Al [4], 1100 Al, Si-saturated Al solid solution, Si, SiC, 6061 Al, and 6061 Al–0.05 and 0.20 SiC whisker systems.

Table I. Average Thermal Expansion of 6061 Al Alloy and SiC Composites from 20°C to the Indicated Temperature on Heating and Cooling (Standard Deviations in Parenthesis)

	$\Delta L/L \times 10^{-3}$				
		6061 Al–SiC composite			
		5% SiC		20% SiC	
T (°C)	6061 Al	Particles	Whiskers	Particles	Whiskers
20	0	0	0	0	0
100	1.62 (0.05)	1.49 (0.05)	1.39 (0.03)	1.17 (0.03)	1.00 (0.04)
200	3.96 (0.05)	3.59 (0.03)	3.30 (0.02)	2.94 (0.04)	2.39 (0.05)
300	6.48 (0.04)	5.97 (0.05)	5.37 (0.04)	4.97 (0.05)	3.83 (0.10)
400	9.26 (0.04)	8.50 (0.26)	7.34 (0.05)	7.01 (0.22)	5.16 (0.05)
500	12.42 (0.06)	11.47 (0.09)	9.47 (0.08)	9.53 (0.17)	6.72 (0.10)
400	9.34 (0.03)	8.54 (0.13)	7.35 (0.09)	7.16 (0.21)	5.07 (0.10)
300	6.54 (0.08)	5.89 (0.13)	5.31 (0.07)	5.14 (0.22)	3.66 (0.04)
200	3.98 (0.04)	3.58 (0.09)	3.35 (0.10)	3.18 (0.16)	2.29 (0.04)
100	1.65 (0.02)	1.45 (0.08)	1.48 (0.09)	1.43 (0.20)	1.05 (0.02)
20	0.10 (0.10)	0.00 (0.01)	0.37 (0.12)	0.32 (0.14)	0.47 (0.14)

volume-average basis and the measurement is $\Delta L/L = 6.72 \times 10^{-3}$ as shown in Table I. The computation demonstrates that there is much more to determining the expansion properties of these composite systems than can be accounted for on a volume-average basis. The missing considerations are mechanical compatibility and geometry of the constituents.

The effects of elastic interaction on thermal expansion properties are well established [8, 9]. Plastic effects are not as fully understood. In the present study, the importance of plastic deformation effects was investigated by measuring the thermal expansion properties of the composite systems over repeated thermal cycles. Previously we have considered the thermally induced effects of combined elastic and plastic deformation behavior on the model expansivity of a pair of concentric spheres for a two-component particle system [1]. Figure 3 shows detailed measurements for the 5 and 20% SiC particle-reinforced 6061 Al composite systems. The 5% composite results are shifted upward in accordance with the internal scale. The total thermal expansion over the 20–500°C interval is given numerically for the first and last cycle at the upper points of the curve. The cumulative permanent deformation obtained at room temperature is given at the origin reached on the final cooling cycle. The 5% SiC particle sample had differences in expansion of $\Delta L/L = 0.16 \times 10^{-3}$ at 500°C on three cycles and negligible permanent deformation after thermal cycling. In contrast to this behavior, the 20% SiC particle composite showed a permanent expansion at 20°C over one cycle of $\Delta L/L = 0.31 \times 10^{-3}$ and for two cycles of $\Delta L/L = 0.47 \times 10^{-3}$. These permanent expansions are approaching the

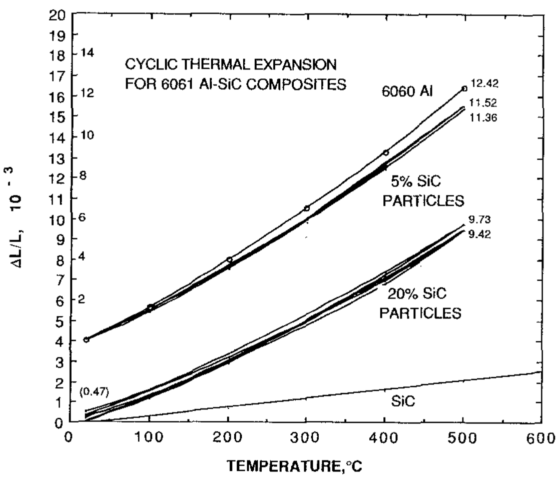

Fig. 3. Cyclic thermal expansion of 6061 Al–0.05 and 0.20 SiC particle systems.

proof strain values used to determine the plastic yield strengths of materials.

The cyclic thermal expansion of the 5 and 20% SiC whisker composites shows much greater permanent strains following the same cycling sequences as indicated in Fig. 4. For example, a total permanent expansion of $\Delta L/L = 1.55 \times 10^{-3}$ over four cycles is obtained for the 5% whisker composite and a $\Delta L/L = 1.40 \times 10^{-3}$ expansion over three cycles of the 20% composite. Average permanent expansions per cycle of $\Delta L/L = 0.39 \times 10^{-3}$ and $\Delta L/L = 0.47 \times 10^{-3}$ apply for the 5 and 20% composites, respectively. An interesting aspect of the permanent deformation obtained at 20°C is that it is produced in each cycle by reduced contraction occurring in the interval from 100 to 20°C. There is no question for these composite systems that the permanent expansions are comparable to the proof strains employed to describe plastic deformation behavior in the bulk straining of materials.

3. MODEL EXPANSIVITIES

The limiting cases of purely elastic interaction compared with totally plastic behavior of two concentric spheres with the outer (matrix) sphere showing linear work hardening were employed to define the bounds on the thermal expansivities of the particulate eutectic Al–Si metallurgical composite system [1]. The thermal expansivity, α_b, at the outer radius, b, of a

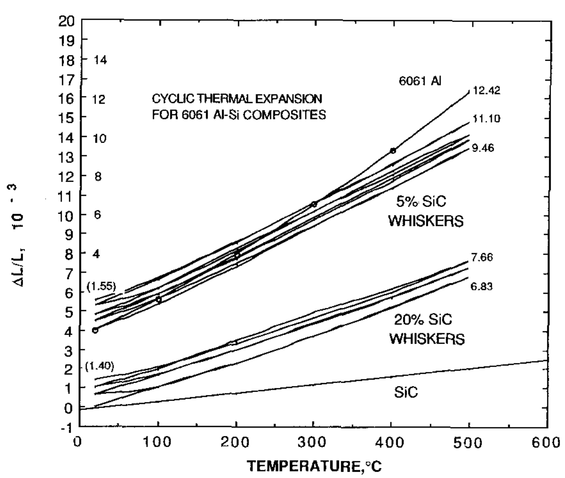

Fig. 4. Cyclic thermal expansion of 6061 Al–0.05 and 0.20 SiC whisker systems.

totally elastic shell of material 2 (Al) containing an inner spherical particle of material 1 (Si) with radius, a, also strained elastically, is obtained as

$$\alpha_b = \alpha_2 - (\alpha_2 - \alpha_1) V_1 \left(\frac{\left(\frac{1}{3K_2} + \frac{1}{4G_2}\right)}{\left\{\frac{1}{3}\left[\frac{1}{K_1} + \left(\frac{1}{K_2} - \frac{1}{K_1}\right) V_1\right] + \frac{1}{4G_2}\right\}} \right) \tag{1}$$

where K and G are the elastic compressibility and shear moduli, respectively, for material 1 or 2. The value of $V_1 = (a/b)^3$. The value of K is connected with Young's modulus, E, and Poisson's ratio, ν, by $K = E/3(1-2\nu)$ and $G = E/2(1+\nu)$. For two materials with identical elastic properties, Eq. (1) reverts to the volume-average rule of mixtures. For the opposite case, when the matrix is totally plastic, a new equation is obtained:

$$\alpha_b = \alpha_2 - (\alpha_2 - \alpha_1) V_1 \left(\frac{\left[3\left(\frac{f}{g}\right)\frac{1}{2E_2}\right]}{\left\{\frac{1}{g}\left(\frac{2m}{1-m}\right)\frac{1}{3}\left[\frac{1}{K_1} + \left(\frac{1}{K_2} - \frac{1}{K_1}\right) V_1\right] + \frac{1}{2E_2}\right\}} \right)$$

$$+ \left(\frac{\left[\frac{2}{3}\left(\frac{1}{g}\right)\left(\frac{\Delta\sigma_y}{\Delta T}\right)\left(\frac{1}{K_2} - \frac{1}{K_1}\right) V_1 \ln\left(\frac{1}{V_1}\right)\right]}{\left\{\frac{1}{g}\left(\frac{2m}{1-m}\right)\frac{1}{3}\left[\frac{1}{K_1} + \left(\frac{1}{K_2} - \frac{1}{K_1}\right) V_1\right] + \frac{1}{2E_2}\right\}} \right) \tag{2}$$

where $\Delta\sigma$ is the change in yield stress accompanying the temperature change ΔT, and f and g are constants related to the linear work hardening of the plastic stress–strain curve of slope mE, in accordance with the equations $f = 1 + [2m/(1-m)][1-\nu_2]$ and $g = 3 + [2m/(1-m)][1+\nu_2]$.

In Eq. (2), with $m = 0 = \Delta\sigma_y/\Delta T$, the rule of mixtures equation for α_b is obtained. For $m = 1.0$, the system is elastic so that the third term in Eq. (2) is omitted, and the remainder of the equation goes over to Eq. (1). Equations (1) and (2) have been applied to computing α_b using the material properties for 6061 Al and SiC in the cases of an elastic matrix and a totally plastic matrix and are shown in Figs. 5 and 6 for the 5 and 20% SiC composites.

In the case of a continuous fiber-reinforced composite, a model similar to the concentric spheres has been utilized for two coaxial cylinders representing the inner fiber and outer matrix [10]. Complicated closed-form mathematical solutions were obtained for the axial and trans-

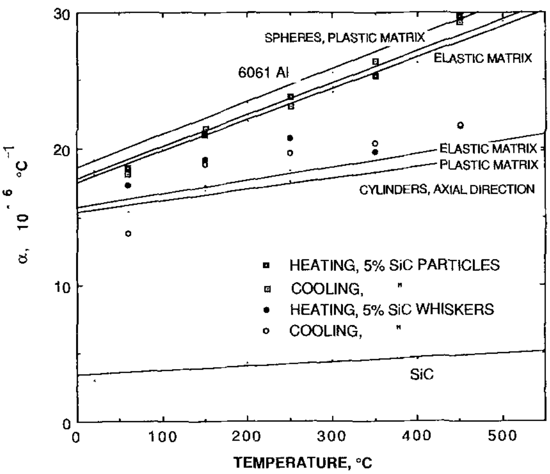

Fig. 5. Thermal expansivities of 6061 Al–0.05 SiC particles or whiskers and computations from the sphere and cylinder models.

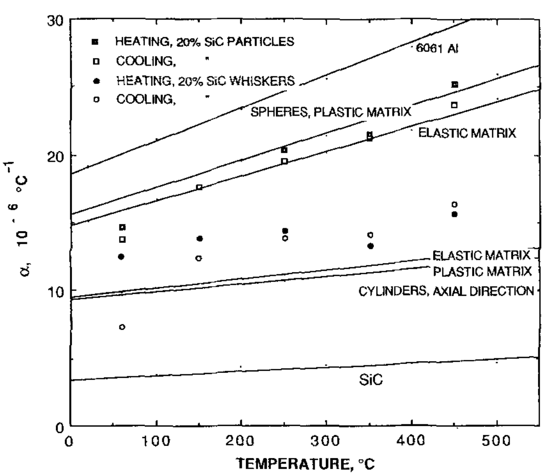

Fig. 6. Thermal expansivities of 6061 Al–0.20 SiC particles or whiskers and computations from the sphere and cylinder models.

verse expansivities and internal stresses. An alternate numerical method of analysis is used for our purposes here.

For cylindrical symmetry, the strains are

$$\varepsilon_r = \frac{du}{dr} = \frac{1}{E}\left[\sigma_r - \nu(\sigma_\theta + \sigma_z)\right] + \varepsilon_r^p + \alpha\,\Delta T$$

$$\varepsilon_\theta = \frac{u}{r} = \frac{1}{E}\left[\sigma_\theta - \nu(\sigma_r + \sigma_z)\right] + \varepsilon_\theta^p + \alpha\,\Delta T \tag{3}$$

$$\varepsilon_z = \frac{dw}{dz} = \frac{1}{E}\left[\sigma_z - \nu(\sigma_r + \sigma_\theta)\right] + \varepsilon_z^p + \alpha\,\Delta T$$

where u and w are the radial and axial displacements, respectively, σ_i are the stresses, and ε_i^p are the plastic strains. The solution for elastic interaction between the cylinders gives σ_z as the intermediate stress, so that according to the Tresca yield criteria, plastic flow will occur in the $r-\theta$ plane. With $\varepsilon_z^p = 0$ and constant volume $\varepsilon_\theta^p + \varepsilon_r^p = 0$.

Considering the equilibrium of stresses [11]

$$\varepsilon_p = \left(\frac{1-m}{m}\right)\frac{(\sigma_\theta - \sigma_r) - \sigma_y}{E_2} \tag{4}$$

The differential equation for the radial displacement is

$$\frac{d^2u}{dr^2} + \frac{1}{r}\frac{du}{dr} - \frac{u}{r^2} = \frac{2\sigma_y}{hE_2' r} \tag{5}$$

where $h = 1 + [m/(1-m)][1-\nu_2^2]$ and $E_2' = E_2/(1+\nu_2)(1-2\nu_2)$. The general solution is

$$u = \frac{\sigma_y}{hE_2'}\, r\ln(r) + Ar + \frac{B}{r} \tag{6}$$

where A and B are constants. The axial displacement is $w = Cz$. The stresses in the outer cylinder are

$$\sigma_{rr}^{(2)} = \frac{\sigma_y}{h}\left[\ln r + (1-\nu_2)\right] + A_2E_2' - 2G_2\frac{B_2}{r^2} + \nu_2E_2'C_2 - 3K_2\alpha_2\,\Delta T$$

$$\sigma_{\theta\theta}^{(2)} = \frac{\sigma_y}{h}\left[\ln r + \nu_2\right] + A_2E_2' + 2G_2\frac{B_2}{r^2} + \nu_2E_2'C_2 - 3K_2\alpha_2\,\Delta T \tag{7}$$

$$\sigma_{zz}^{(2)} = \frac{2\nu_2\sigma_y}{h}\left[\ln r + \frac{1}{2}\right] + 2\nu_2E_2 + (1-\nu_2)\,E_2'C_2 - 3K_2\alpha_2\,\Delta T$$

The inner cylinder is assumed to remain elastic. This requires that the radial displacement is finite. Therefore, $u_1 = A_1 r$, where A_1 is a constant, and the stresses are

$$\begin{aligned}\sigma_{rr}^{(1)} &= A_1 E_1' + \nu_1 E_1' C_1 - 3K_1 \alpha_1 \Delta T \\ \sigma_{\theta\theta}^{(1)} &= A_1 E_2' + \nu_1 E_1' C_1 - 3K_1 \alpha_1 \Delta T \\ \sigma_{zz}^{(1)} &= 2\nu_1 A_1 E_1' + (1-\nu_1) E_1' C_1 - 3K_1 \alpha_1 \Delta T\end{aligned} \tag{8}$$

The boundary conditions are $\sigma_{rr}^{(2)} = 0$ at $r = b$ and at $r = a$, $u_1 = u_2$, $w_1 = w_2$, and $\sigma_{rr}^{(1)} = \sigma_{rr}^{(2)}$. The balance of forces gives $\int_0^a \sigma_{zz}^{(1)}\, dA_1 + \int_a^b \sigma_{zz}^{(2)}\, dA_2 = 0$. With these total equations and boundary conditions, a linear set of equations for the dependent variables A_1, A_2, B_2, and $C_1 = C_2$ can be solved. Separate cases of elastic deformation of the matrix and of plastic deformation of the matrix with linear strain hardening have been considered. The calculated constants were then employed to calculate stresses and displacements, which in turn were used to calculate the axial and transverse expansivities. The axial expansivities for the 6061 Al–SiC composites are shown in Figs. 5 and 6 for the 5 and 20% SiC composites, respectively.

Figure 5 shows the model computed expansivities in comparison with those values determined from the expansion data given in Table I for the 5% SiC particle or whisker composite. There is very good agreement between the computed model expansivities and the experimental results obtained for the 5% SiC particle composite. Important deviations do occur at the lowest and highest temperatures. The shift in measurements obtained from the heating and cooling cycles matches approximately the shift between the fully elastic case and the perfectly plastic matrix. Less agreement between the model calculations and the experimental results is shown for the 5% SiC whisker system. Two reasons for the difference are that the model calculations are for an infinite, continuous fiber, leading to an underestimation of expansivity and the first occurrence here of significant permanent deformation effects. Despite these concerns, Fig. 6 shows reasonable agreement between the model and the experimental expansivities for the 20% SiC particle and the whisker composites. Better agreement occurs for the particle composite as expected. Again, the whisker composite model calculations for the continuous fiber fall below the measurements. The largest range in measured expansivities occurs for the low-temperature determinations, as indicated in the expansion figures themselves.

4. SUMMARY

Measurements have been made of the expansion properties over the temperature interval from 20 to 500°C of composites of 6061 Al–SiC particle or whisker systems containing 5 or 20% SiC by volume. The addition of low-expansion SiC to 6061 Al alloy reduces the total composite expansion more than can be accounted for on a volume-average basis. The aligned SiC whiskers have a much larger influence on reducing the expansion than do particles. For example, the 5% whiskers give approximately the same reduced expansion as the 20% particles. The generation of internal stresses is undoubtedly responsible for the expansion effects which have been observed.

REFERENCES

1. T. A. Hahn and R. W. Armstrong, *Int. J. Thermophys.* **9**:179 (1988).
2. C. T. Liu and J. Gurland, *Trans. ASM* **58**:66 (1965).
3. T. A. Hahn and R. W. Armstrong, in *Thermal Expansion 7 (Seventh Symposium)*, D. C. Larsen, ed. (Plenum Press, New York, 1982), p. 195.
4. R. O. Simmons and R. W. Balluffi, *Phys. Rev.* **34**:52 (1960).
5. R. J. Arsenault, *Mater. Sci. Eng.* **64**:171 (1984).
6. ASTM, *Annual Book of ASTM Standards, E 228 (71), Standard Test Method* (ASTM, Philadelphia, 1980), p. 1041.
7. T. A. Hahn and R. K. Kirby, in *Thermal Expansion 1971 (Third Symposium)*, M. G. Graham and H. E. Hagy, eds. (Am. Inst. Phys. Conf. Proc., 1972), p. 87.
8. R. A. Schapery, *J. Comp. Mater.* **2**:280 (1968).
9. K. Wakasshima, M. Otsuka, and S. Umekawa, *J. Comp. Mater.* **8**:391 (1974).
10. T. A. Hahn, *Thermal Expansion Behavior and Analysis for Al–Si Eutectic Alloys and the Composite Material Systems: Al–SiC and Al–W.* Ph.D. dissertation (University of Maryland, College Park, 1986).
11. Y. Y. Earmme, W. C. Johnson, and J. K. Lee, *Met. Trans. ASM* **12A**:1521 (1981).